Using SC-FDMA Waveform in a Shared Spectrum Context with High Efficiency

Benjamin Ros, Sonia Cazalens, Christelle Boustie
Satellite telecommunications systems department
CNES (French Space Agency)
18 avenue E. Belin
31400 Toulouse, France
e-mail: {benjamin.ros, sonia.cazalens, christelle.boustie}@cnes.fr

Xavier Fouchet
SILICOM
12 rue Caulet
31300 Toulouse, France
e-mail: xfouchet@silicom.fr

***Abstract*—The trend for future communication systems is the efficient sharing of frequency bands on one hand (Cognitive Radio) and the emergence of satellite/terrestrial integrated systems, which is a topic of interest in 5G research process, on the other hand. All this is in order to optimize the management of the spectrum. Single-Carrier Frequency Division Multiple Access (SC-FDMA) is well suited waveform for satellite link thanks to its low Peak-to-Average Power Ratio (PAPR) level. Its Orthogonal Frequency-Division Multiplexing (OFDM) based transmitter architecture, allowing a granular frequency access, reinforces its ability to perform well in shared spectrum context. More generally, SC-FDMA waveform seems to be a good candidate for both fixed-mobile convergence and satellite-terrestrial hybridization. This article aims to demonstrate two main points. Firstly, it will be proved that SC-FDMA waveform, even with holes enabling a dynamic use of the spectrum, is well suited to cope with satellite payload impairments, such as nonlinear amplifier and Input Multiplexer. Secondly, it will be assessed that doing frequency holes does not degrade so much air interface performance by using surboost of remaining carriers. As a whole, in this paper, the relevance of SC-FDMA in a shared spectrum context is demonstrated.**

Keywords-shared spectrum; integrated satellite terrestrial system; intentional jammer; (Extended and Weighted) Single-Carrier Frequency Division Multiple Access; amplifier non linearity; Input Multiplexer.

I. INTRODUCTION

Preliminary study results on insertion of frequency holes in Single-Carrier Frequency Division Multiple Access (SC-FDMA) waveform for a satellite system have been published in [1]. Complementary results are presented here.

Multi-carrier waveform is not historical waveform used on satellites. But, as European Union is promoting through incoming 5G integration of satellite and terrestrial components, paradigm is currently being modified [2]. Indeed, to make easier spectrum scalability, satellite should be able to choose sub-bands it uses depending on existing terrestrial systems. Moreover, in the case of integrated systems specifically, to encourage mass market terminal deployment, terminal should be able to receive the satellite signal or terrestrial one with the same chipset. This emphasizes the need for satellite to use a multi-carrier granular access, as it is already the case in terrestrial systems. The high crest factor of OFDM does not allow optimizing the efficiency of satellite amplifiers. An intermediate solution is the use of SC-FDMA. On forward link, its interest has already been demonstrated in the Digital Video Broadcasting (DVB) - Next Generation broadcasting system to Handheld (NGH) standardization process in S-band mobile system [3]. This waveform is also recommended in an International Telecommunication Union (ITU) working group for satellite International Mobile Telecommunications-Advanced (IMT-Advanced) systems [4]. More recently, interest of this waveform raised in European Telecommunications Standards Institute - Satellite Communication and Navigation (ETSI-SCN) and DVB - Second Generation Satellite Extensions (S2x) standardization process applicable to high frequency bands (Ku, Ka), especially for broadband systems.

In Section II, a brief state of the art is presented. In Section III, the considered scenarios are described. In Section IV, description of SC-FDMA waveform enabling frequency holes is done. Methodology used to analyze obtained results is introduced, with first simulation results. In Section V, performances with satellite payload impairments are discussed. In Section VI, impact of surboost on the air interface is studied before giving further work horizon in Section VII.

II. BRIEF STATE OF THE ART

In terrestrial context, a variant of OFDM known as non-contiguous OFDM (NC-OFDM) has been proposed for Cognitive Radio networks [5]. It allows the transmission of information in presence of primary users, by deactivating the subcarriers already occupied to avoid interferences. Efficient implementation of NC-OFDM transceiver has been proposed. It is based on an FFT pruning algorithm, which allows reducing the execution time [6]. Nevertheless, one major drawback of OFDM is its high Peak-to-Average Power Ratio (PAPR). SC-FDMA waveform allows reducing this PAPR, while still having the properties of frequency agility. Previous studies have demonstrated that Non-

Contiguous (NC) SC-FDMA can generally achieve better performance than NC-OFDM [1][7]. Some issues appears in the literature relative to the employment of non-contiguous multicarrier-modulation-based data transmission systems, like out of band interference, power amplification, synchronization, implementation complexity [8][9], but always in a terrestrial context.

In this paper, satellite scenarios and channels are considered: effects of satellite payload on NC-SC-FDMA are studied, as well as a mean to compensate loss of bandwidth by using power of unused subcarriers.

III. CONSIDERED SCENARIOS

Two main application cases have an interest. On the one hand, an integrated system example (the spectrum of the terrestrial and satellite components is managed by the same company) is given in Figure 1. It provides a service to nomadic or mobile devices. To optimize the spectrum usage according to the traffic, the scheduler decides if a part of the band is allocated to either satellite component or terrestrial one. On the other hand, a satellite system use frequency bands allocated to terrestrial systems provided it does not cause harmful interference. To enable good reception of satellite signal by satellite terminals, system operator may decide to null signal in the band where a certain amount of terminals are jammed, as it is depicted on Figure 2.

IV. SC-FDMA WAVEFORM MODELISATION WITH FREQUENCY HOLES

Firstly, the SC-FDMA modeling is described and waveform power fluctuations properties are analyzed. Then we explain how to insert frequency holes. The model of interference used is described. We present a method to compare the waveforms and finally, reference simulations are showed.

A. Basic SC-FDMA modeling

Because there have been several studies on SC-FDMA waveform, model will not be strictly detailed [10][11]. However, differences with OFDMA transceiver architecture will be emphasized. General SC-FDMA transceiver is summarized in Figure 3, and is described hereafter.

Firstly, interleaved and coded bits b_n are mapped into symbols c_i, $i \in [0, \dots, M-1]$. Spreading operation, specific to SC-FDMA transmission, is then done by applying an M–Discrete Fourier Transform (DFT) to the c_i symbols to get C_k symbols, $k \in [-\frac{M}{2}, \dots, \frac{M}{2} - 1]$:

$$C_k = \frac{1}{\sqrt{M}} \sum_{i=0}^{i=M-1} c_i \, e^{-j\frac{2\pi ki}{M}} \qquad (1)$$

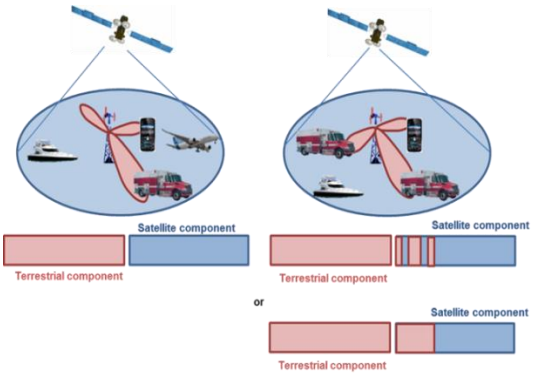

Figure 1. Example of integrated system managing efficiently its spectrum.

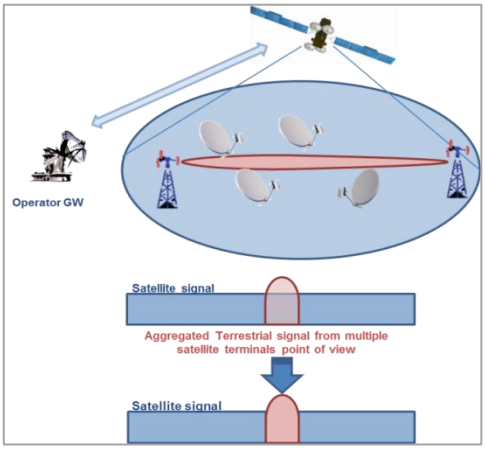

Figure 2. Example of satellite system using cognitive radio to transmit efficiently its signal.

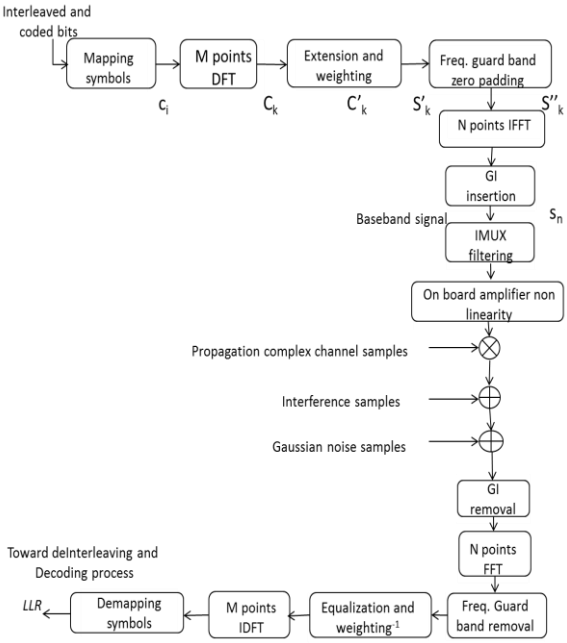

Figure 3. SC-FDMA transceiver architecture.

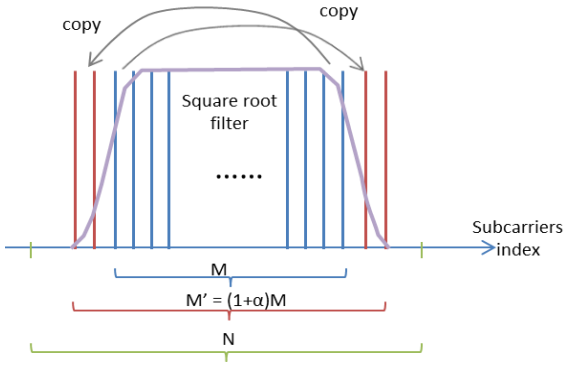

Figure 4. Extension and weighting process.

In the case of EW-SC-FDMA, as it can be seen in Figure 4, some of the edge C_k symbols are duplicated and put at the opposite side edge in the guard band. Main sizing parameter here is α, called the roll off factor. Extension process outputs M' (equals to $(1+\alpha)M$) complex symbols C_k'. Weighting process is finally applied over these subcarriers in order to have a square root raised cosine shaping [10]. It multiplies term by term $H_{SRC}(k')$ with C_k' to get S_k'.

Note that $H_{SRC}(k')$, $k' \in \left[-\frac{M'}{2}; +\frac{M'}{2}-1\right]$, is the frequency response of the square root raised cosine filter, given by:

$$H_{SRC}(k') = \begin{cases} 1, & 0 \le |k'| < \frac{(1-\alpha)}{2}M \\ \cos\left[\frac{\pi}{2\alpha M}\left(|k'| - \frac{(1-\alpha)}{2}M\right)\right], & \frac{(1-\alpha)}{2}M \le |k'| < \frac{(1+\alpha)}{2}M \end{cases} \quad (2)$$

It can be pointed out that when α equals to 0, process is strictly equivalent to SC-FDMA process. Next, unused subcarriers in the guard band are filled by zero, exactly $N - (1+\alpha)M$, to get a vector owning N complex symbols, $S_{k''}$. Note that to be compliant with OFDMA process, N should be a power of 2, which is not the case for M. Lastly, OFDMA modulation process can be done by applying an N-Inverse Fast Fourier Transform (IFFT) and inserting guard interval, getting baseband signal s_n.

For receiver considerations, the equalization should use a Minimum Mean Square Error (MMSE) frequency domain algorithm, working subcarrier by subcarrier [10][11]. Applied to SC-FDMA waveform (left hand side formula) and EW-SC-FDMA waveform (right hand side formula), estimated symbol $\widehat{x_k}$ is expressed hereafter:

$$\hat{x}_k = \frac{\hat{h}_k^*}{\left|\hat{h}_k\right|^2 + \hat{\sigma}^2} y_k \qquad \hat{x}_k = \frac{\hat{h}_k^* y_k + \hat{h}_{k+M}^* y_{k+M}}{\left|\hat{h}_k\right|^2 + \left|\hat{h}_{k+M}\right|^2 + \hat{\sigma}^2} \quad (3)$$

$\hat{h}_{k(+M)}$ are channel estimates in the useful bandwidth (M equals to 0) or extended bandwidth (M greater than 0). $y_{k(+M)}$ are received complex symbols after OFDM FFT matched filter. $\hat{\sigma}^2$ is the noise power estimate in a subcarrier bandwidth, that is to say Rs divided by the size of OFDM FFT, where Rs is I/Q sampling frequency.

Furthermore, a slightly difference that can be observed with SC-FDMA receiver compared to OFDMA one, is the way to compute the Log Likelihood Ratio (*LLR*) metrics at the demapping symbols step. Classic *LLR* formulation is reminded here:

$$LLR(b_i) = ln \frac{\sum_{x \in c_i^1} exp\left(-\frac{|I - \rho_I I_x|^2 + |Q - \rho_Q Q_x|^2}{2\sigma^2}\right)}{\sum_{x \in c_i^0} exp\left(-\frac{|I - \rho_I I_x|^2 + |Q - \rho_Q Q_x|^2}{2\sigma^2}\right)}, \quad (4)$$

where $x = I_x + jQ_x$ is a symbol of the Quadrature amplitude modulation (QAM) constellation, c_i^j represents the symbols of the constellation carrying the bit b_i when b_i equals to j, I and Q are the in phase and quadrature components of the received signal after OFDM FFT process, $\rho_{I/Q}$ is the fading on the I or Q component, $2\sigma^2$ is the Additive White Gaussian Noise (AWGN) variance, I_x and Q_x denote the reference symbols of the QAM constellation. In SC-FDMA receiver, because of the despreading process, i.e., there is a M points Inverse-DFT between equalization and demapping process, it is assumed that $\rho_{I/Q}$ can be approximated to the root mean square of the frequency channel response of the corresponding OFDMA symbol over the active subcarriers $H_c(k')$:

$$\rho_{I/Q} \approx \sqrt{\frac{\sum_{k'=-M'/2}^{\frac{M'}{2}-1} |H_C(k').H_{SRC}(k')|^2}{M}}. \quad (5)$$

B. *Waveform power fluctuations properties*

Because dealing with non-linearity effects, the study of envelope fluctuations for each waveform may help to understand further results. This is why complementary cumulated density function for instantaneous power is given for each studied waveform in Figure 5. As it can be found in literature, SC-FDMA waveform performs better than OFDMA one. Using extension can help to better decrease fluctuations. However, one shall note that this comparison is considering waveforms without frequency holes insertion.

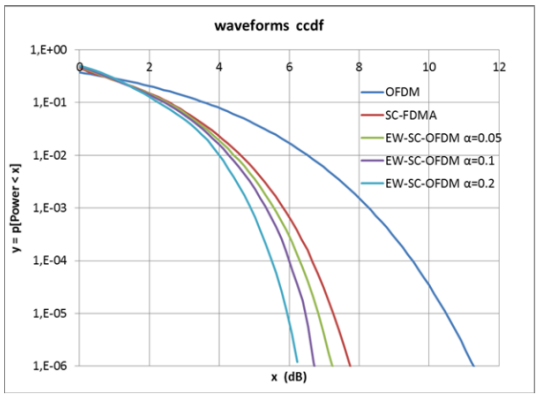

Figure 5. Complementary Cumulated Density Function of waveforms intantaneous power. 512 sub-carriers are used for simulations.

C. Frequency holes insertion

Frequency holes are inserted inside useful signal at the spreading process level. In fact, spreading applies a $L<M$ DFT over the incoming c_i symbols before filling M-L other symbols with zero, as it is drawn in Figure 6. Some vocabulary is necessary to define where frequency hole is located. β is defined as the relative bandwidth occupied by frequency holes over maximum achievable useful bandwidth:

$$\beta = \frac{M-L}{M}. \quad (6)$$

Δ is the relative shift of the frequency hole center relatively to the bandwidth center. To clarify these notations, an example is given in Figure 7.

D. Interference model

The interferer location is defined as it is done for the frequency holes, with β and Δ parameters. Generative model is quite simple: complex symbols are generated according to a normal law $\mathcal{N}(0;\beta)$, supposing power of the useful signal as unitary power when occupying all possible subcarriers. Interference symbols are applied to subcarriers as if it was an OFDMA signal. When frequency holes are defined, interferences are added exactly at the holes location.

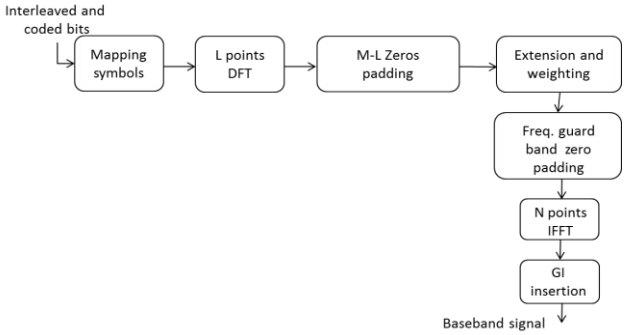

Figure 6. SC-FDMA transceiver architecture enabling frequency holes.

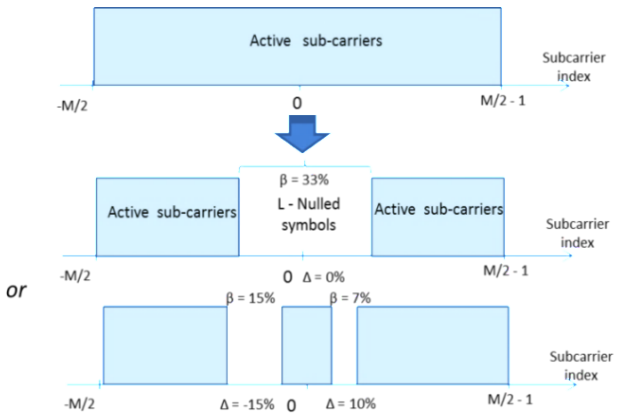

Figure 7. Position and size example of a frequency hole.

E. Comparative method analysis

We are about to compare different waveforms enabling creation of a frequency hole inside their spectrum. Here is proposed a method to compare waveforms, considering power loss, signal quality loss, and Carrier over Intermodulation ratio. *Power loss* corresponds to *OBO* value, and *Signal quality loss* equals to the performance gap considering non-linearity sub-block or not. *Total loss* metric is then defined as (all the quantities are in dB):

$$Total\ loss = Signal\ quality\ loss + Power\ loss$$

$$\begin{cases} power\ loss = |OBO| \\ signal\ quality\ loss = \left(\frac{C'+I_m}{N}\right)_{BER=10^{-5}} - \left(\frac{C}{N}\right)_{BER=10^{-5}} \end{cases} \quad (7)$$

where $\left(\frac{C}{N}\right)_{BER=10^{-5}}$ is the required signal to noise ratio in dB with ideal amplifier response at the bit error rate (*BER*) of 10^{-5}, and $\left(\frac{C'+I_m}{N}\right)_{BER=10^{-5}}$ is the required amplified signal power (pure signal plus intermodulated part) to noise ratio in dB at *BER* 10^{-5}. Both metrics are given at the receiver input location (see Figure 8). Assuming that I_m has a Gaussian behavior, pure Signal to Intermodulation power ratio $\left(\frac{C_I}{I_m}\right)$ can be derived (linear form):

$$\left(\frac{C'}{I_m}\right) = \frac{1 + \left(\frac{C'+I_m}{N}\right)_{BER=10^{-5}}}{\left(\frac{C}{N}\right)^{-1}_{BER=10^{-5}} * \left(\frac{C'+I_m}{N}\right)^{-1}_{BER=10^{-5}} - 1} \quad (8)$$

Signal to Intermodulation power ratio is an important criterion according to satellite operators, because it demonstrates the ability of the payload to work with any spectral efficiency. Indeed, a low $\left(\frac{C_I}{I_m}\right)$ ratio results in degradation of total $\left(\frac{C}{N+I}\right)$ ratio, and then limitation of spectral efficiency. As a result, performances of the waveforms will be compared at equal $\left(\frac{C'}{I_m}\right)$ ratio. It shall be pointed out that for a same spectral efficiency, $\left(\frac{C'}{I_m}\right)$ is directly linked to the signal quality loss considering (7) and (8). Thus, judicious representation may be, for each waveform, required $|OBO|$ to get *BER* = 10^{-5} vs $\left(\frac{C'}{I_m}\right)$ representation.

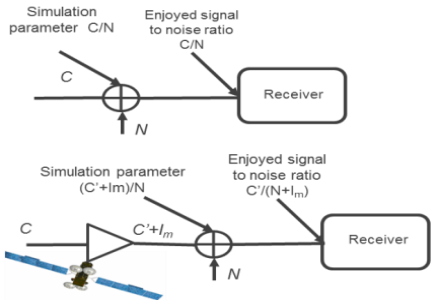

Figure 8. Receiver input signal to noise ratio, with/without non-linearity.

F. Reference simulations

The simulations are performed by using a DVB-NGH like transceiver chain [1]. DVB-NGH specifications enable SC-FDMA utilization without extension and weighting functionality. Besides, frequency hole, IMUX filtering, on-board nonlinear amplifier and interferences had to be considered as it is depicted in Figure 9. A significant importance should be given to the way how signal to noise ratios are computed when dealing with frequency holes. As power at output of the amplifier is unitary in simulations, it was chosen to decrease signal power with the same bandwidth reduction ratio. It enables comparing results at the same Es/N0. This decrease of signal power will be cancelled for simulations demonstrating of the surboosting effect benefits. Lastly, the simulation parameters are summarized in Table I.

V. STUDY OF SATELLITE PAYLOAD IMPAIRMENTS

Satellite payload impairments models usually include three main origins: nonlinear amplifier, selective input filters and phase noise.

For the current work, non-linearity effects and input filtering effects are considered separately. Phase noise is not considered because it is well known that effect is very weak over a Quadrature Phase Shift Keying (QPSK) modulation combined with current stability specifications over satellite local oscillators.

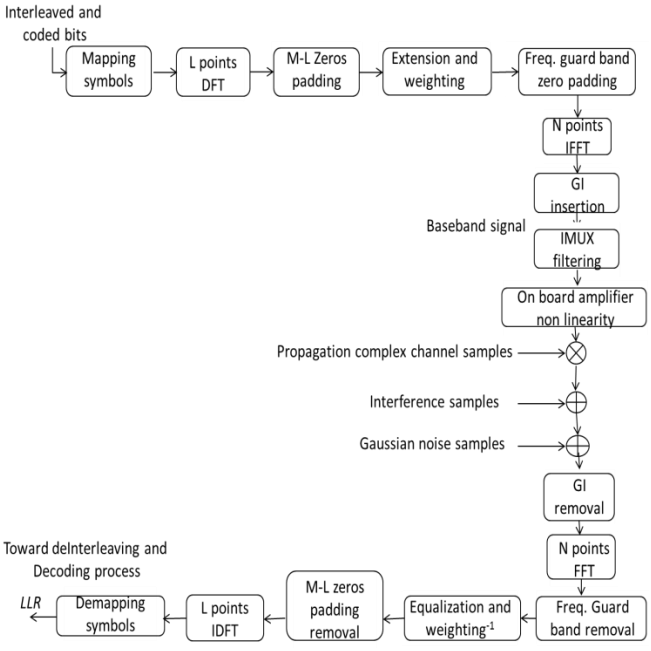

Figure 9. Simulation Chain, including SC-FDMA, frequency hole, interference and non linearity functionalities.

Input filters distortion may have an effect over the performances, but as the three studied waveforms (OFDMA, SC-FDMA, EW-SC-FDMA) have a subcarrier equalization process, it can be expected that the effect will be quite close in all cases, while not negligible. This is the reason why it was decided to focus on non-linearity effects, knowing there are envelope fluctuations differences between waveforms.

In the simulation tool, IMUX filtering is first applied to the baseband signal, before being processed by the nonlinear conversion. Signal passed through satellite amplifier, having a unitary power, is applied to propagation channel block, as it is shown in Figure 10.

TABLE I. MAIN PARAMETERS FOR PERFORMED SIMULATIONS

Parameter name	Value
Satellite signal Bandwidth	15 MHz
Sampling frequency Rs	120/7 MHz
I/Q sample duration	58.33 ns
Modulation and coding	QPSK 2/3 LDPC + BCH encoder 16200 bits codeword
Max active subcarriers (M)	426
OFDM FFT size (N)	512
OFDM Guard interval	1/16
Total OFDM symbol duration	31.73 µs
SC-FDMA	α = 0 (SC-FDMA) or α = 5% (EW-SC-FDMA)
Frequency hole insertion	Δ=0, β=33% when activated
Interference insertion	By default not activated. Δ=0, β=33% when activated
IMUX filtering	By default not activated
Satellite RF model	MTV by default.
Propagation channel	Ideal (AWGN) in this study

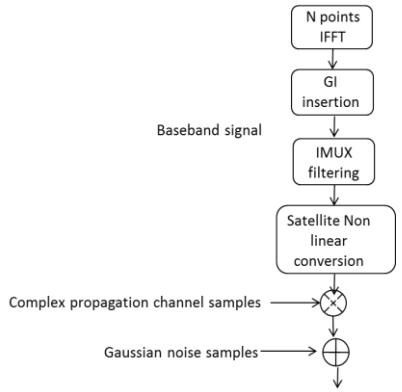

Figure 10. Insertion of non-linearity conversion and IMUX filtering in the transceiver.

A. *Nonlinear amplifier*

A typical model is chosen, called Mobile Television (MTV) model, giving Output Back Off (*OBO*) [dB] as a function of Input Back Off (*IBO*) [dB]. This model was chosen because it seemed to be quite realistic. Another model has been considered, NGH model, because it was used in DVB-NGH standardization process. As it seemed to be less realistic (especially phase characterization), it has not been used as a baseline. See on Figure 11 the non-linearity conversion curves of these amplifiers.

As a reference, *BER* simulations have been performed according to the method described previously. For a wide range of C/I_m, it appears in Figure 12 that SC-FDMA like waveforms outperform OFDMA in terms of *OBO* vs C/I_m, with a gap increasing when C/I_m is growing.

These results emphasize the fact that when no interferer is present, SC-FDMA is a good choice to be compatible with terrestrial multi-carrier legacy and to enjoy efficient use of satellite payload. For these reference simulations, the results with NGH amplifier have also been considered (see Figure 13). Conclusions about the interest of SC-FDMA are the same as with MTV amplifier, but with worse performances in required *OBO* at low C/I_m.

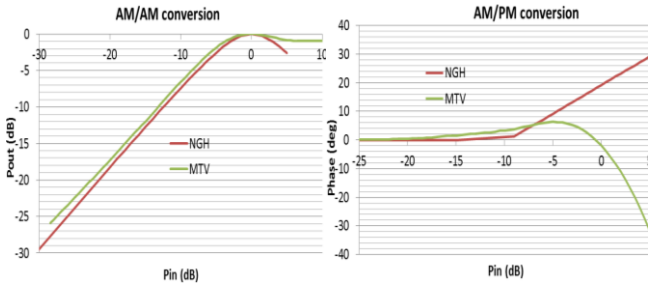

Figure 11. Non linearity conversion curves of MTV and NGH amplifiers.

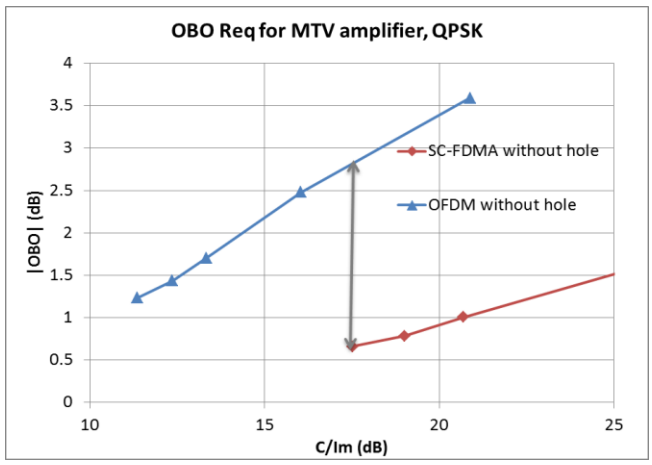

Figure 12. Comparison of waveforms in terms of OBO vs C/I_m when no frequency holes are inserted and without interference, for MTV amplifier.

Here, frequency hole was inserted with default parameters (Δ=0 and β=33%). Especially for single carrier waveforms, inserting such wide hole inside useful bandwidth may modify its fluctuations behavior. But, as it is depicted in Figure 14, single carrier waveforms performances are not so much degraded by the hole insertion, and remain quite competitive compared to OFDM, despite the large width of the hole. About OFDM results, it can be pointed out that results with and without frequency hole are quite similar. This can be explained by the multi-carrier effect of OFDM: multicarrier signal split in two parts remains a multi-carrier signal. This is the reason why in the following, only SC-FDMA waveform will be considered.

The influence of hole size was studied for SC-FDMA modulation (see Figure 15). It can be noted that for all hole sizes, between 2 and 50% width, a degradation of 0.5 dB on average has been observed.

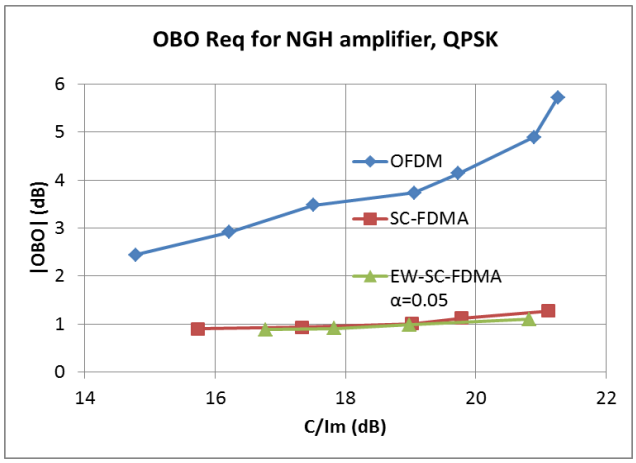

Figure 13. Comparison of waveforms in terms of OBO vs C/Im when no frequency holes are inserted and without interference, for NGH amplifier.

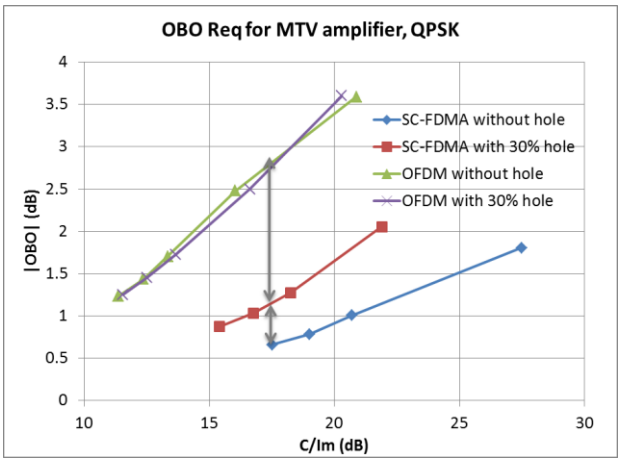

Figure 14. Comparison of waveforms in terms of OBO vs C/I_m when frequency holes are inserted.

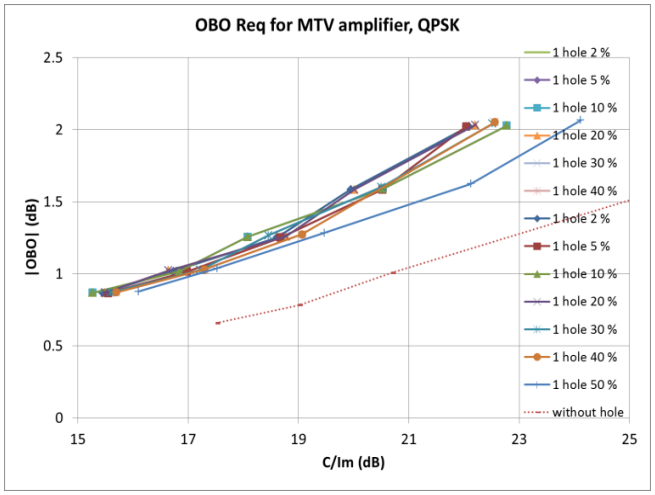

Figure 15. SC-FDMA performances in terms of OBO vs C/I_m with one frequency hole.

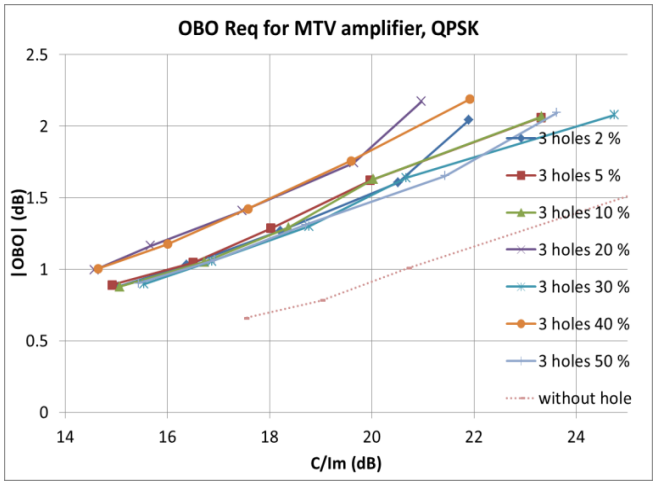

Figure 16. SC-FDMA performances in terms of OBO vs C/I_m with 3 frequency holes.

For integrated systems or satellite systems, which share frequency bands or have to deal with jammers, it could happen that several holes would be needed to avoid interference effects. Therefore, simulations have been performed with 3 holes, centered in $\Delta = [-27\%, 0\%, +27\%]$. Results can be seen in Figure 16, where percentile value means the total width of the frequency holes relatively to the useful bandwidth. Two sets of curves can be observed; first pack, closer than without hole performance curve, shows around 0.5 dB *OBO* degradation compared to without hole. This degradation is almost the same as single hole performance for SC-FDMA. For 3 holes, some combinations of width and holes positions make appear an additional degradation. Indeed, intermodulation power spectrum density is not similar to white Gaussian noise, which is frequency flat. Therefore, when useful signal is in front of intermodulation peak, it brings a bit more degradation.

B. *Input Multiplexer*

Input Multiplexer (IMUX) filter templates are given in Figure 17. Two filters are considered for the study, having a different cut-off frequency: first one has its 3 dB cutting-off frequency at 0.42 sampling frequency, where the second one is cutting-off at 0.5 sampling frequency. Both filters have a group delay greater than 800 ns, corresponding to more than thirteen times the *I/Q* symbol duration (see Table I).

In a satellite payload, IMUX filter is designed to split different incoming channels before amplifying them separately or by group. Because it is very important to filter noise and adjacent channels contribution, IMUX filters are usually designed with a margin on the channel bandwidth, in order to ensure that signal is not decreased at band edges, and to prevent group delay interferences effects at band edges also. This is the reason why two filters are considered for the simulations: aim is to demonstrate that SC-FDMA waveform enables extending signal bandwidth up to filters shoulders without losses, thanks to cyclic prefix adding up signal replicas.

As it is written in Table I, number of active OFDM subcarriers is 426, whereas OFDM FFT size is 512. It brings that occupied bandwidth relatively to *I/Q* symbol rate Rs is 0.84. That is to say signal is located between +/- 0.42 Rs. Thus, when using 0_5 filter as an IMUX, only group delay may have an impact on performances because filter has very weak fluctuations in the useful frequency band. Besides, using 0_42 filter, band edges of the signal are faded by the filter, so that it would be expected an additional degradation.

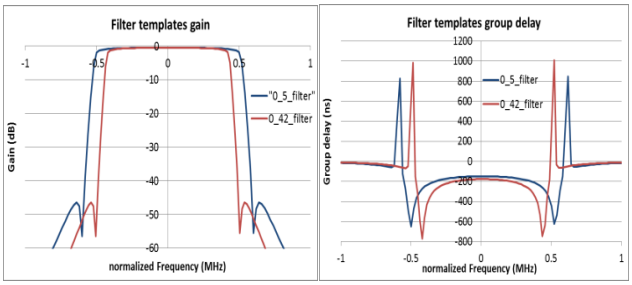

Figure 17. IMUX filter templates models : 0_42_filter and 0_5 filter.

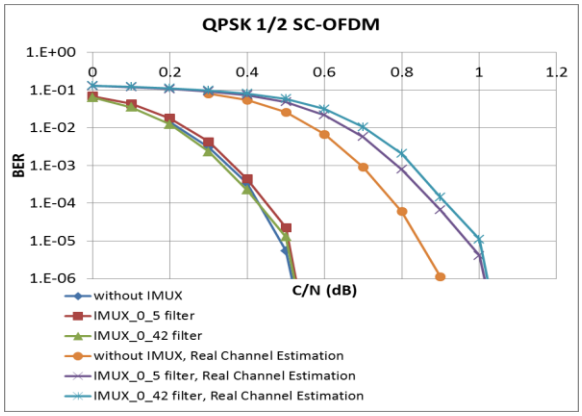

Figure 18. IMUX filter effect over SC-FDMA performances.

In this case study, simulations have been performed with and without real channel estimation, in order to assess real impact of IMUX filtering on receiver performances (see Figure 18). Results in QPSK ½ show that with perfect channel estimation, both filters have no impact over performances, whereas there is 0.1 dB degradation in real channel estimation, with respect to no IMUX insertion. This result demonstrates that multicarrier waveform helps filling at its best available bandwidth.

C. *Effects of interferences*

Interferences are inserted with Δ=0 and β=33% parameters. In addition, NGH amplifier was used for these simulations. Modulation and coding scheme is QPSK ½. I_0, the power spectrum density of interferer is the same as C_0, the power spectrum density of the signal.

That leads to relatively weak level of interferers but with quite large bandwidth (1/3 of achievable useful bandwidth). With no real surprise, it is first checked that inserting hole in any of the three frequency granular access waveforms results in a negligible degradation (see Figures 19, 20 and 21), because only secondary lobes of interferences are captured by active useful subcarriers when frequency hole is inserted.

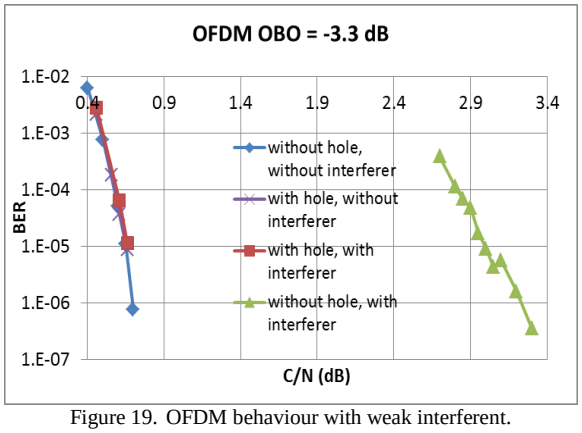

Figure 19. OFDM behaviour with weak interferent.

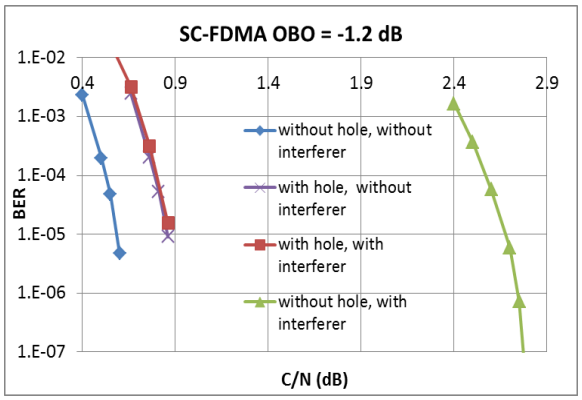

Figure 20. SC-FDMA behaviour with weak interferent.

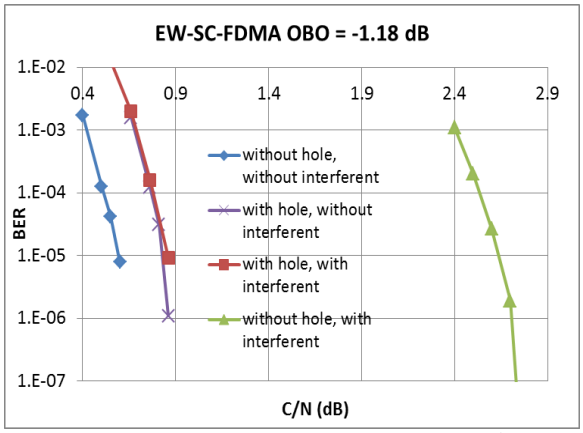

Figure 21. EW-SC-FDMA behaviour with weak interferent.

Besides, no creating hole when interferer is present is showing quite degraded results, even if the interferer has a weak level. Reader shall point out that weak interferer was chosen to visualize the degradation on the same curve. But, from a system point of view, power spectrum density of a terrestrial interferer would be greater than satellite useful signal one, and would emphasize the need for such frequency hole in the waveform.

VI. IMPACT OF SURBOOST ON PERFORMANCES

For this case study, satellite amplifier is providing constant power, whether or not frequency holes are present. Therefore, when a frequency band is unused, delivered power spreads in remaining useful sub-carriers. It creates a surboost of ratio η compared to baseline transmission:

$$\eta = \frac{BW_N}{BW_N - BW_H}, \quad (9)$$

BW_N is the useful nominal bandwidth, BW_H is the bandwidth corresponding to frequency hole.

The aim of this section is to demonstrate that surboost can compensate, from a bit rate point of view, useful bandwidth decrease by increasing spectral efficiency of the transmission. The steps of the process are given below. First, for different couples of modulation and coding schemes (MODCOD), compute frequency hole width in order to compensate, on a linear channel with a surboost η, required E_S/N_0 rising due to the changing of MODCOD (see Table II) [12]. Secondly, considering 3 frequency holes, searching *OBO* working point to reach *OBO* near from 17 dB, for both MODCOD of a couple. Lastly, compare for both MODCOD required Es/N_0 and associated bit rate.

Results are presented in Figure 22. The bit rate is computed considering MODCOD efficiency and overhead item such as pilot and frame building insertion, guard interval and a useful bandwidth of 14.2 MHz, according to Table I parameters [3].

TABLE II. MODULATION AND CODING SCHEMES COUPLES FOR SURBOOSTING EFFECT DEMONSTRATION

MODCOD 1, without hole and surboost	MODCOD 2, with hole and surboost	Frequency hole cumulated width (1-1/η)
QPSK ½ (4/9 real)	QPSK 3/5	32.4%
16QAM 4/5	16QAM 5/6	11.5%

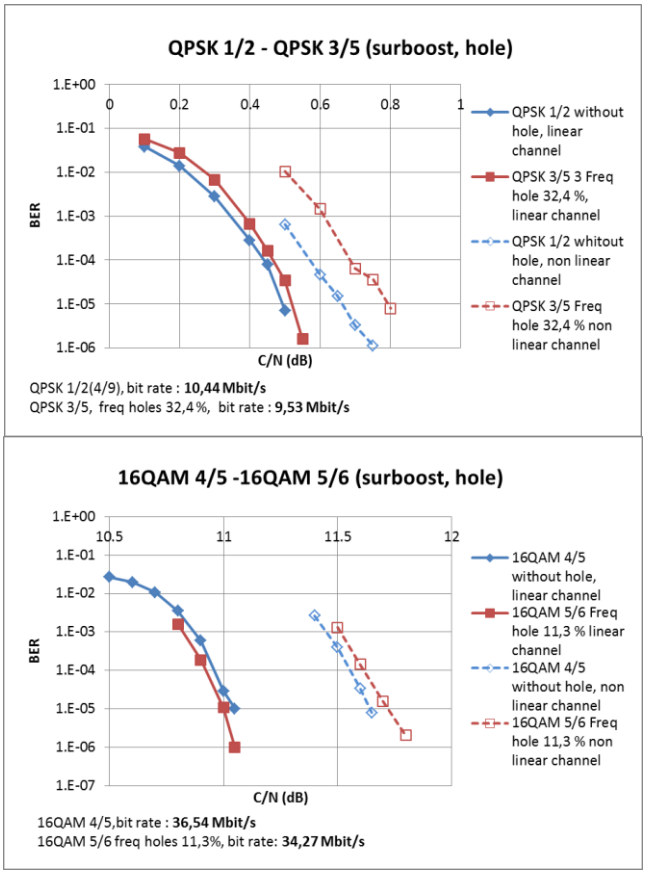

Figure 22. Using of the surboost to balance frequency hole insertion for two MODCOD couples.

Full line curves show that for linear channel, frequency hole width has been correctly chosen to balance E_S/N_0 requirement difference between two MODCOD. In dotted line, the same simulations over non-linear channel are performed. Lastly, physical layer input bit rate for two MODCOD show that the loss of bandwidth is worse than the loss of the bit rate thanks to the spectral efficiency increase.

VII. CONCLUSION AND FUTURE WORK

At a time where, on one hand, there is a need to make easier spectrum scalability and on the other hand, manufacturers are working to maximize the payload efficiency, a SC-FDMA based solution was introduced to address this issue. In this paper, it has been shown that SC-FDMA waveform fluctuations enable using satellite payload in an efficient way, and that creating frequency hole do not degrade so much air interface performances; SC-FDMA waveform remains in all cases relevant compared to OFDMA. Thus, using this waveform would take advantage of both frequency scalability and payload efficiency, while offering a solution at physical layer level for dynamic spectral resource sharing systems.

For further work, others topics should be processed. Standard modification impact of the introduction of frequency holes in the signal appears to be the first subject. Next, an accurate modeling of interferer would help to prove that frequency holes are enough to avoid interference effects. More generally, a cooperation with a satellite system manufacturer would be needed to assess the impact of using SC-FDMA at onboard level (amplifiers working point, signal routing) and ground level (terminal design, resource access methods).

ACKNOWLEDGMENT

The authors thank the Satellite Mobile Innovative Laboratory and Engineering project of French Space Agency allowing applicative research on such waveforms.

REFERENCES

[1] B. Ros, X. Fouchet, S. Cazalens, and C. Boustie, “SC-FDMA Waveform Enabling Frequency Holes in a Shared Spectrum Context,” IARIA SPACOMM 2015 : The Seventh International Conference on Advances in Satellite and Space Communications, Barcelona, Spain, April 2015, pp. 1-6, ISBN: 978-1-61208-397-1.

[2] 5G-Private Public Partnership project homepage. [Online]. Available from: <http://5g-ppp.eu/etp/> 2015.11.06

[3] ETSI, “Digital Video Broadcasting (DVB); Next Generation broadcasting system to Handheld, physical layer specification (DVB-NGH),” EN 303 105 V1.1.1, May 2013.

[4] ITU-R, Recommendation M.2047-0, “Detailed specifications of the satellite radio interfaces of International Mobile Telecommunications-Advanced (IMT-advanced),” December 2013. [Online]. Available from: <http://www.itu.int/dms_pubrec/itu-r/rec/m/R-REC-M.2047-0-201312-I!!PDF-E.pdf> 2015.11.06

[5] H. Tang, “Some physical layer issues of wide-band cognitive radio systems,” 2005 First IEEE International Symposium on New Frontiers in Dynamic Spectrum Access Networks, Baltimore, USA, Nov. 2005, pp.151-159, ISBN: 1-4244-0013-9.

[6] R. Rajbanshi, A.M. Wyglinski, and G. J. Minden, “An efficient implementation of NC-OFDM transceivers for cognitive radios,” 2006 First International Conference on Cognitive Radio Oriented Wireless Networks and Communications, Mykonos Island, June 2006, pp. 1-5, ISBN: 1-4244-0381-2.

[7] H. Gao, "Comparison of SC-FDMA and NC-OFDM schemes for cognitive radio networks," 2010 Second International Conference on Computational Intelligence and Natural Computing, Wuhan, Sept. 2010, ISBN: 978-1-4244-7705-0.

[8] H. Bogucka, A.M. Wyglinski, S. Pagadarai, and A. Kliks, "Spectrally agile multicarrier waveforms for opportunistic wireless access," IEEE Communications Magazine Vol. 49, Issue 6, June 2011, pp. 108-115, DOI: 10.1109/MCOM.2011.5783994.

[9] H. Bogucka, P. Kryszkiewicz, and A. Kliks, "Dynamic Spectrum Aggregation for Future 5G Communications," IEEE Communications Magazine Vol. 53, Issue 5, May 2015, pp. 35-43, DOI: 10.1109/MCOM.2015.7105639.

[10] S. Okuyama, K. Takeda, and F. Adashi, "MMSE frequency-domain equalization using spectrum combining for Nyquist filtered broadband," 2010 IEEE 71st Vehicular Technology Conference, Taipei, Taiwan, May 2010, pp. 1-5, ISBN: 978-1-4244-2518-1.

[11] H. Kobayashi, T. Fukuharal, H. Yuant, and Y. Takeuchi, "Proposal of single carrier OFDM technique with adaptive modulation method," The 57th IEEE Semiannual Vehicular Technology Conference, April 2003, pp. 1915-1919, vol. 3, ISBN: 0-7803-7757-5.

[12] ETSI, "Digital Video Broadcasting (DVB); Implementation guidelines for a second generation digital terrestrial television broadcasting system (DVB-T2)," TS 102 831 V1.2.1, August 2012.